Nonconformal Interaction Models and Thermodynamics of Polar Fluids

Edgar Ávalos and Fernando del Río*

Departamento de Fısica, Universidad Autónoma, Metropolitana, Iztapalapa, Apdo 55 534

Santiago Lago

Departamento de Ciencias Ambientales, Universidad Pablo de Olavide, Sevilla 41013, Spain

Received: July 22, 2004; In Final Form: October 14, 2004

In this work, we develop a simple potential model for polar molecules which represents effectively and accurately the thermodynamics of dilute gases. This potential models dipolar interactions whose nonpolar part is either spherical, as in Stockmayer (SM) molecules, or diatomic, as for 2-center Lennard-Jones molecules (2CLJ). Predictions of the second virial coefficient for SM and polar 2CLJ fluids for various dipole moments and elongations agree very well with results of recent numerical calculations by C. Vega and co-workers (*Phys. Chem. Chem Phys.* **2002**, *4*, 3000). The model is used to predict the critical temperature of Stockmayer fluids for variable dipole moment and is applied to HCl as an example of a real polar molecule.

1. Introduction

Research efforts to elucidate the properties of polar fluids have been spurred by the ubiquity of polar substances as solvents in laboratory and industry and by the challenge of dealing with the anisotropy and relatively long range of the dipolar interaction. Work on the statistical mechanics of polar fluids has proceeded alongside liquid-state theory for many decades.[2−4] Recent developments can be identified along two broad research lines: The first explores mainly structural properties of polar fluids in a wide variety of conditions, such as ferroelectric structures,[5,6,] fluids in confined geometries,[8,9] liquid-crystalline phases,[10−12] and dimerizing off-centered linear molecules.[13] A second line has focused on predicting thermodynamic properties of "realistic" polar fluids and in modeling these properties by means of analytic expressions.[14−17] An ultimate goal in this molecular thermodynamics approach is to generate theoretically based equations of state applicable to real polar substances. This work aims to contribute along this line of inquiry.

In this paper we develop a novel way to build accurate effective interactions for polar fluids. These potentials lead to closed-form expressions of thermodynamic properties and to quantitative estimates of the effects of molecular features on those properties. This method is closely related to the approach of "mapping" of properties.[18] Effective potentials have been used by different authors to provide simplified models of more complex systems. This approach may be used e.g. to incorporate three-body effects[19,20] within a two-body spherical potential or to model the effect of the solvent in a solution.[21,22] The simpler effective potentials are then used to estimate thermodynamic properties by means of integral equations or simulations. Another role of effective interactions is closer to the use of reference potentials in perturbation theory. In this approach, also referred to as "mapping" , a single model system such as the hard-sphere or square-well fluid furnishes a unified basis to express the properties of many different systems.[23,18] The specifics of a given fluid of interest is then imbedded into the potential parameters, usually state-dependent. In this sense, an effective potential u_{ef} of a pure system with intermolecular potential u, is defined such as to reproduce accurately a specific thermodynamic property via a chosen statistical mechanical expression. If the chosen quantity is the pressure P and having specified a particular way of expressing it, e.g. by Clausius virial, u_{ef} is then defined such that

$$P(\rho, T; [u_{ef}]) \cong P(\rho, T; [u]) \tag{1}$$

holds to good approximation. From this definition, u_{ef} will in general depend on the state—density ρ and temperature T—on the property chosen—the pressure P—and on the choice of expression for P. In this work we deal mostly with density *independent* potentials, but a word of caution may be in order. The fact that u_{ef} depends in general on density may lead to difficulties[24] that, nonetheless, can be overcome if care is taken when handling u_{ef} in different contexts.[25,26] For instance, if a given u_{ef}—with a particular ρ dependence—has been found to satisfy (1), the appropriate u_{ef} to use in some other property, e.g., the Helmholtz free energy, must have a different dependence on ρ. It has been shown that, for most properties of interest, the different functional forms can be obtained one from each other.[27]

Of course, to be of practical or theoretical value, u_{ef} has to be simpler in form than the interaction u it effectively represents. Some years ago, a particularly successful class of spherical—but nonconformal—model potentials was introduced to represent effectively and accurately interactions of many real substances in the gaseous phase. These model potentials are handled by means of the "approximate nonconformal (ANC) theory" introduced as a rigorous extension of the principle of corresponding states.[28,29] In this work we develop ANC effective potential models for polar fluids and exhibit some of their uses. Besides the usual molecular energy and size, the ANC theory introduces a third molecular parameter s to account for the form of the potential profile; s is called the softness of the potential. The three ANC potential parameters are then the energy ϵ, the molecular diameter r_m measured at the potential minimum and the softness s. The ANC potential takes the simple form of a (slightly modified) Kihara potential with spherical core. This

10.1021/jp046735y CCC: $30.25
Published on Web 12/07/2004

theory leads to a closed form for the second virial coefficient $B(T)$ and with constant parameters (ϵ_0, r_{m_0}, s_0) has been very successful in reproducing $B(T)$ within experimental error for a wide class of substances: Noble gases, homodiatomics, *n*-alkanes and *n*-perfluoroalkanes (up to C_8H_{18} and C_7F_{16}) and several hetero- and polyatomics, some of these slightly polar like CO and NO. Many binary mixtures of the former substances have also been accounted for.[30−32] To our knowledge, there is no unified approach that matches the range and accuracy of the ANC approach in dealing with the thermodynamics of dilute real substances. More recently, the ANC theory has been extended to liquids and viscosity coefficients, achieving good agreement with simulation results of dense fluids[33] and with experimental viscosity coefficients of dilute real substances.[34] These developments mean that ANC potentials provide a very convenient path to thermodynamic properties. Nevertheless, in its present state the theory has failed to account for properties of strongly polar fluids such as alcohols, even in the gaseous phase.

Given the importance of polar substances, it is the purpose of this work to breach this deficiency by providing accurate effective potentials for various models of polar molecules. It has been suggested by Müller and Gelb[35] that this kind of isotropic potential may be sufficient to treat fluids at relatively high temperatures. We show how to build model potentials which are useful also at low or moderate temperatures. Their usefulness in the gaseous phase is exemplified by giving closed-form expressions for $B(T)$ of a wide class of polar models recently obtained numerically. An estimate of the change in critical temperature with dipolar strength of Stockmayer fluids and a prediction of the virial coefficient of HCl, based on experimental critical properties, are also given as illustrations. Application to other real dilute polar gases and to dense fluids will be the subject of forthcoming publications.

The pair potential energy will be assumed to be the sum of a nonpolar kernel φ_K—accounting for overlap and dispersion forces—and a dipolar term φ_{DD}. The simpler type of model is the generalized Stockmayer (SM) with a spherical $\varphi_K(r)$ of the modified Kihara form that includes as a special case the standard SM function for a Lennard-Jones (LJ) 12−6 kernel $\varphi_{LJ}(r)$. A second choice for kernel is a 2-centered LJ (2-CLJ) potential, which could be a better model for real polar molecules. As a matter of fact, C. Vega et al. have calculated recently and systematically $B(T)$ of polar molecules with a 2-CLJ kernel[1] results that have a direct bearing on this work. For the standard SM model we should mention computer simulations of its vapor−liquid equilibrium,[36−38] which will be used to test one of the predictions of this work.

The scheme of the paper is as follows. Section 2 surveys briefly ANC theory. Section 3 deals with the generalized SM models, their effective potentials, and the corresponding expressions for $B(T)$, shown to predict accurately the numerical data.[1] In section 4 the approach is applied to the dipolar 2-CLJ molecule with parallel and oblique dipole to the molecular axis; for the parallel case, $B(T)$ is predicted with excellent agreement with the numerical values. The two examples of application of the results of this work are illustrated in section 5. Conclusions are given in the final section.

2. Approximate Nonconformal Theory

The main features of the ANC theory relevant to this paper are described here, the interested reader may consult the original references for more detail.[28,29] ANC theory introduces a family of spherical potentials φ_{ANC} with minimum at $r = r_m$ of depth

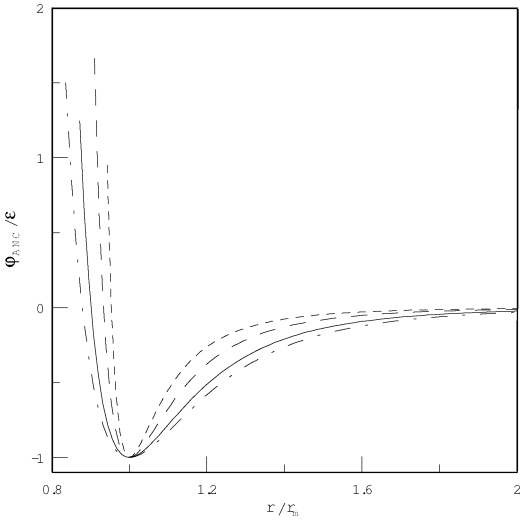

Figure 1. Potential $\varphi_{ANC}(z)$ against $z = r/r_m$ for different values of the softness s. The solid line stands for the reference $s = 1.0$. Two harder potentials are $s = 0.5$ (short dashes) and $s = 0.7$ (long-dashes); the softer case $s = 1.2$ (dash−dotted line) is also shown.

ϵ; the softness s is the molecular parameter accounting for the form of the potential profile.[29] The ANC potential has the modified Kihara form

$$\varphi_{ANC}(z; \epsilon, s) = \epsilon\left\{\left[\frac{1-a}{\zeta(z,s)-a}\right]^{12} - 2\left[\frac{1-a}{\zeta(z,s)-a}\right]^{6}\right\} \quad (2)$$

where $\zeta(z, s) = (1 + (z^3 - 1)/s)^{1/3}$, $z = r/r_m$, and r is the center-to-center distance between the particles. The minimum of φ_{ANC} is at $z = 1$ and $\varphi_{ANC}(1) = -\epsilon$. The function $\varphi_1(z) = \varphi_{ANC}(z, s = 1)$, used as a reference, has the spherical Kihara form with a as hard-core diameter. Further, taking $a = 0.0957389$ makes $\varphi_1(z)$ closely conformal to the pair potential of argon.[30] The softness s in eq 2 determines the profile of $\varphi_{ANC}(z, s)$ against z. Let a potential of interest be $\varphi(r)$ with minimum $-\epsilon$ at $r = r_m$. Also let $z_1(\varphi)$ and $z(\varphi)$ be the inverses of $\varphi_1^*(z) = [\varphi_1(z) + \epsilon]/\epsilon$ and $\varphi^*(z) = [\varphi(z) + \epsilon]/\epsilon$ respectively, the local softness $S(\varphi = \varphi_0)$ is then given by the ratio

$$S(\varphi_0) = \left(\frac{\partial z^3}{\partial \varphi^*}\right)_{\varphi=\varphi_0} \Big/ \left(\frac{\partial z_1^{\,3}}{\partial \varphi^*}\right)_{\varphi=\varphi_0} \quad (3)$$

From (3) $S(\varphi_0)$ is inversely proportional to the slope of φ^* against z^3 at the distance $z(\varphi_0)$. Varying s alters the shape of $\varphi_{ANC}(z, s)$ in a very simple way, illustrated in Figure 1: decreasing s narrows the potential well, i.e., makes it steeper or harder, and conversely, increasing s widens the well. Any two potentials with the same $S(\varphi)$ are conformal to each other. When $S(\varphi) = s =$ constant, ANC theory gives an exact linear relation between the second virial coefficients of the substance $B^*(T^*)$ and of the reference $B_1^*(T^*)$:[28]

$$B^*(T^*) = 1 - s + sB_1^*(T^*) \quad (4)$$

where $B^*(T^*) = B(T)/(2\pi r_m^3/3)$, $T^* = kT/\epsilon$. Although in general S does depend on φ it is found that (4) holds to a good approximation when s is taken as the average of $S(\varphi)$ over an appropriate energy range.[28] Further, when $\varphi(z, \Omega)$ depends on the intermolecular orientation Ω, the local softness $S(\varphi)$ in (3) depends also on Ω but (4) holds again approximately if s is taken as the angle average of $S(\Omega)$. In all these cases, when $S(\varphi, \Omega)$ is substituted by a single constant s and (4) is used,

one talks of the one-*s* approximation. A second-order approximation considers a different constant softness in the attractive and repulsive regions of (2). When analyzing theoretical models the two-*s* approximation is some times necessary, but in its application to real substances the one-*s* approximation has been found sufficient to reproduce $B(T)$ within experimental error for many substances.[39] The effective potentials for polar substances have been developed both in the one-*s* and the two-*s* approximations; the latter is detailed in Appendix A.1.

3. The Generalized Stockmayer Potential

In this section we deal with generalized SM potentials (GSM) consisting of a spherical kernel plus a dipole−dipole interaction; partial preliminary results have been communicated previously.[40] We show that the angular dependence in φ_{GSM} is eliminated by integrating over orientations and that the resulting sphericalized potential may be replaced by φ_{ANC} with the appropriate parameters. The sphericalization procedure is similar to that used by Hirschfelder et al.[41] and here we only quote the main results. Details can be found in Appendix A.2.

The GSM potential is simply the sum of an ANC potential φ_{ANC} with parameters ϵ_0, r_{m0}, and s_0 plus the interaction φ_{DD} between two permanent dipoles of moment μ, that is

$$\varphi_{GSM}(z, \Omega) = \varphi_{ANC}(z; \epsilon_0, s_0) + \varphi_{DD}(z, \Omega; \mu_0^*) \qquad (5)$$

where $z = r/r_{m0}$ and $\mu_0^{*2} = \mu^2/\epsilon_0 r_{m0}^3$ and $\varphi_{DD}(z, \Omega; \mu_0^*)$ is given in Appendix A.2. The reduced second virial coefficient $B^* = B/(2\pi r_{m0}^3/3)$ and $T_0^* = kT/\epsilon_0$ is then given by

$$B^*(T_0^*) = \frac{1}{8\pi}\int_\Omega d\Omega \int_{z=a}^{\infty} dz \frac{\partial}{\partial z}\left\{\exp\left[-\frac{\varphi_{GSM}(z, \Omega; \mu_0^*, s_0)}{\epsilon_0 T_0^*}\right]\right\} z^3 \qquad (6)$$

where $d\Omega \equiv \sin\theta_1\, d\theta_1\, \sin\theta_2\, d\theta_2\, d\phi$. The sphericalized dipolar interaction $\varphi_{DD}^{sphe}(z)$ is now defined as

$$\exp[\varphi_{DD}^{sphe}(z)/\epsilon_0 T_0^*] = \frac{1}{8\pi}\int d\Omega\, \exp[\varphi_{DD}(z, \Omega; \mu_0^*)/\epsilon_0 T_0^*]$$

that from Appendix A.2 is given by

$$\varphi_{DD}^{sphe}(z) = -\epsilon_0 T_0^* \ln \sum_{m=0}\left\{\frac{G_m}{(2m)!}[\mu_0^{*4}/T_0^{*2} z^6]^m\right\} \qquad (7)$$

where the constants G_m are given by (A.6). Thus, if the original potential φ_{GSM} is replaced by

$$\varphi_{GSM}^{sphe}(z) = \varphi_{ANC}(z; \epsilon_0, s_0) + \varphi_{DD}^{sphe}(z; \epsilon_0, T_0^*, \mu_0^*) \qquad (8)$$

then, inverting the order of integration in (6), $B^*(T_0^*)$ is exactly given by

$$B^*(T_0^*) = \int_{z=a}^{\infty} dz \frac{\partial}{\partial z}\left\{\exp\left[-\frac{\varphi_{GSM}^{sphe}(z; T_0^*, \mu_0^*, s_0)}{\epsilon_0 T_0^*}\right]\right\} z^3 \qquad (9)$$

This relation shows that φ_{GSM}^{sphe} is an exact effective potential, in the sense already defined, because it gives the same thermodynamic property, $B(T)$, as the original $\varphi_{GSM}(z, \Omega)$. Actually, $B(T)$ can be calculated analytically for the GSM potential, with $s_0 = 1$. An outline of the method and the result obtained are given also in Appendix A.2.

3.1. Introducing an Effective Potential. 3.1.1. Generalized Stockmayer Model. In this section, we extract the effect of the dipole interaction from $\varphi_{GSM}^{sphe}(z)$ for the standard SM fluid—i.e. taking $s_0 = 1$ and $a = 0$. It is also shown that $\varphi_{SM}^{sphe}(z)$ may be replaced by a simpler $u_{ef}(z)$ to very good accuracy. The fact that B^* depends on three independent variables T_0^*, μ_0^*, and s_0 makes it necessary to use a class of nonconformal functions as effective potentials. Indeed, this is needed even for a constant s_0 such as the standard SM function.

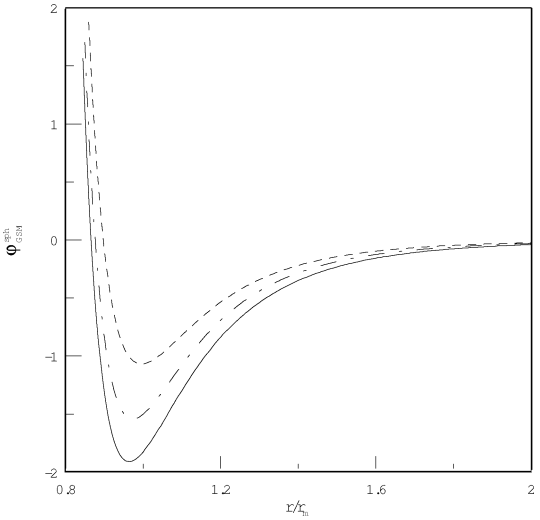

Figure 2. Temperature dependence of the total sphericalized potential $\varphi_{GSM}^{sphe}(z)$. The lines correspond to a GSM with $\mu_0^* = 1.0$ and $s_0 = 1.0$ at $T_0^* = 0.3$ (continuous line), $T_0^* = 0.6$ (dash−dotted line), and $T_0^* = 5.0$ (short dashes).

To analyze the effect of the DD interaction on φ_{GSM}^{sphe}, we assume that $\mu_0^{*2}/T_0^* < 1$ and truncate the sum in (7) to get

$$\varphi_{DD}^{sphe}(z) = -\epsilon_0 T_0^* \ln\left[1 + \frac{\mu_0^{*4}}{3z^6 T_0^{*2}} + \frac{\mu_0^{*8}}{25 z^{12} T_0^{*4}} + ...\right] \qquad (10)$$

where we have used that $G_0 = 1$, $G_1 = 2/3$ and $G_2 = 24/25$. Assuming that $\mu_0^{*4}/T_0^{*2} < 1$, expanding to order μ_0^{*8}/T_0^{*4} gives

$$\varphi_{DD}^{sphe}(z) \cong \epsilon_0 T_0^*\left(-\frac{1}{3}\frac{\mu_0^{*4}}{z^6 T_0^{*2}} + \frac{7}{450}\frac{\mu_0^{*8}}{z^{12} T_0^{*4}}\right) \qquad (11)$$

whose term of order z^{-6} is the Keesom potential.[43] Series of this type have been analyzed by Massih and Mansoori for fluid mixtures.[42]

3.1.2. Standard Stockmayer Model. The standard SM potential is obtained from $\varphi_{GSM}(z, \Omega)$ by making $s_0 = 1$ and $a = 0$, that is

$$\varphi_{SM}^{sphe}(z) = u_{LJ}(z; \epsilon_0) + \varphi_{DD}^{sphe}(z; T_0^*, \mu_0^*) \qquad (12)$$

where u_{LJ} is the well-known Lennard-Jones potential. The effect of adding $\varphi_{DD}^{sphe}(z)$ to a kernel $\varphi_K(z)$ can be appraised from Figure 2: $\varphi_{GSM}^{sphe}(z)$ has its minimum of depth ϵ_{ef} at $r = r_{ef}$. Increasing μ_0^* or decreasing T_0^* makes ϵ_{ef} larger and r_{ef} smaller. Substituting (11) in (12) and collecting terms, we find

$$\varphi_{SM}^{sphe}(z) \cong \epsilon_0\left[\left(1 + \frac{7}{450}\frac{\mu_0^{*8}}{T_0^{*3}}\right)\frac{1}{z^{12}} - 2\left(1 + \frac{1}{6}\frac{\mu_0^{*4}}{T_0^*}\right)\frac{1}{z^6}\right] \qquad (13)$$

Inspection of (13) shows that $\varphi_{SM}^{sphe}(z)$ may be replaced by an effective potential of the Lennard-Jones form:

$$u_{ef}(z_{ef}) = \epsilon_{ef}(z_{ef}^{-12} - 2\, z_{ef}^{-6}) \tag{14}$$

where $z_{ef} = z/r_{ef}$ and with minimum at $z_{ef} = 1$. To make $\varphi_{SM}^{sphe}(z) = u_{ef}(z_{ef})$, r_{ef} and ϵ_{ef} must satisfy

$$\epsilon_{ef} = \epsilon_0\left[1 + \frac{\mu_0^{*4}}{3T_0^*} + \left(\frac{1}{2} - \frac{7}{25T_0^*}\right)\frac{\mu_0^{*8}}{18T_0^{*2}}\right] \tag{15}$$

and

$$r_{ef} = r_{m0}\left[1 - \frac{\mu_0^{*4}}{36T_0^*} + \left(\frac{1}{24} + \frac{1}{25T_0^*}\right)\frac{7\mu_0^{*8}}{108T_0^{*2}}\right] \tag{16}$$

The only approximation made thus far is the truncation in (11).

Equations 15 and 16 confirm that the dipolar interaction effectively increases ϵ_{ef} and reduces r_{ef}, an effect that is much more noticeable for ϵ_{ef} than for r_{ef}. Figure 3 shows ϵ_{ef}/ϵ_0 and r_{ef}/r_{m0} for various μ_0^* and $0.3 < T_0^* < 10$. The range of applicability of (16) can be widened by constructing a simple (1,1) Padé approximant. In this approximation, $\varphi_{SM}^{sphe}(z)$ is strictly conformal to $u_{LJ}(z)$, which explains the LJ form of u_{ef}. Numerical calculation with more terms of (10) shows that $\varphi_{SM}^{sphe}(z)$ differs from conformality with $u_{LJ}(z)$ by a negligible amount within the ranges of μ_0^* and T_0^* considered.

3.1.3. Effective Potential for the Generalized Stockmayer Model. We go back now to the generalized SM potential and take the kernel's softness $s_0 \in (0.50, 1.00)$, the range found for nonpolar real substances.[29] From $\varphi_{GSM}^{sphe}(z)$ we compute the parameters of an effective $u_{ef}(z; \epsilon, r_m, s)$ that is well represented by an ANC function, (2). As in the SM case, the parameters depend T_0^* and μ_0^* but now they also depend on s_0. We thus introduce the functions f_r, f_ϵ, and f_s:

$$\epsilon = \epsilon_0\, f_\epsilon(T_0^*, \mu_0^*, s_0) \tag{17}$$

$$r_m = r_{m0}\, f_r(T_0^*, \mu_0^*, s_0) \tag{18}$$

and

$$s = s_0\, f_s(T_0^*, \mu_0^*, s_0) \tag{19}$$

The minimum of $\varphi_{GSM}^{sphe}(z)$ was localized by differentiation at fixed μ_0^*, s_0 and T_0^* for $\mu_0^* \in (0.0, 1.0)$ and $T_0^* \in (0.3, 10)$. For a given (μ_0^*, s_0, T_0^*), the values of ϵ and r_m, and hence f_ϵ and f_r, were determined. In view of (15) and (16), we assumed

$$f_\epsilon = 1 + C_1\mu_0^{*4}/T_0^* + C_2\mu_0^{*8}/T_0^{*2} \tag{20}$$

and

$$f_r = 1 + C_3\mu_0^{*4}/T_0^* + C_4\mu_0^{*8}/T_0^{*2} \tag{21}$$

The dependence of the C_i on s_0 was found to a good approximation to be linear

$$C_i = c_{i0} + c_{i1}s_0 \tag{22}$$

where the constants $c_{i,j}$ are given in Table 1. The resulting behavior of (20) and (21) with μ_0^* and T_0^* is very similar to that in (15) and (16) except for their dependence on s_0. Figures 4 and 5 show f_ϵ and f_r as functions of $\mu_0^{*4}/T_0{}^*$ for $s_0 = 0.5$, 0.7, 1.0, and 1.1315. The same figures show, for comparison, the analytic approximations to the standard SM case (15) and (16) for variable μ_0^* and $T_0^* = 1.0$. This last case is, as it should be, very close to the GSM result with $s_0 = 1.1315$.

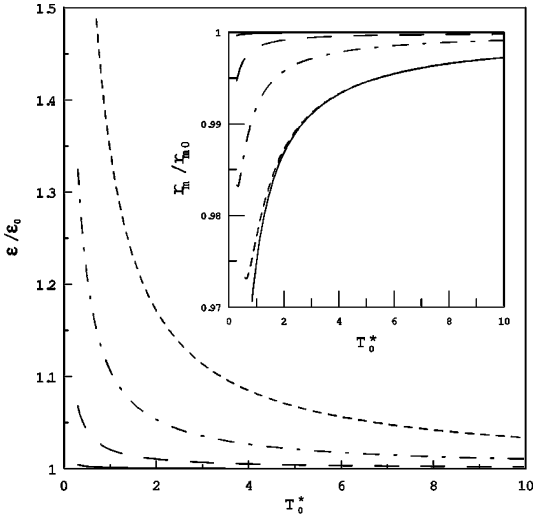

Figure 3. Temperature dependence of the relative depth ϵ/ϵ_0 and relative diameter r_m/r_{m0} (inset) for the standard SM interaction according to eqs 15 and 16. The lines correspond to: $\mu_0^* = 0.5$ (long dashes), $\mu_0^* = 0.75$ (dashes and dots) and $\mu_0^* = 1.0$ (short dashes). The solid lines correspond to ϵ/ϵ_0 for $\mu_0^* = 0.25$ and, in the inset, to a (1,1) Padé approximant to (16) for $\mu_0^* = 1.00$.

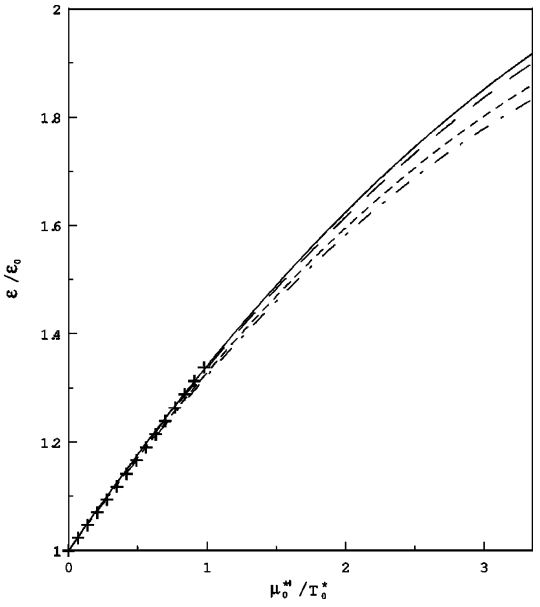

Figure 4. Relative potential depth $\epsilon/\epsilon_0 = f_\epsilon$ for the generalized SM interaction as a function of μ_0^{*4}/T_0^*. The lines correspond to different softnesses: $s_0 = 0.5$ (dashes and dots), $s_0 = 0.7$ (short dashes), $s_0 = 1.0$ (long dashes), and $s_0 = s_{LJ} = 1.1315$ (continuous line). The symbols (+) show values for the standard SM case (analytic approximation) at $T_0^* = 1.0$, which is close to the $s_0 = s_{LJ}$ line.

TABLE 1: Coefficients c_{ij} in Eq 22 Determining the Factors f_ϵ and f_r Defined in Eqs 20 and 21

j	$i = 1$	$i = 2$	$i = 3$	$i = 4$
0	0.011898	−0.002073	0.3422	−0.03393
1	−0.03355	0.005708	0.023 73	0.004851

To find the form of the potential profile we rescale φ_{GSM}^{sphe} with $r_{ef} = r_m$ and $\epsilon_{ef} = \epsilon$ given by (17) and (18)

$$\psi(z_{ef}) = \varphi_{GSM}^{sphe}(z = z_{ef})/\epsilon \tag{23}$$

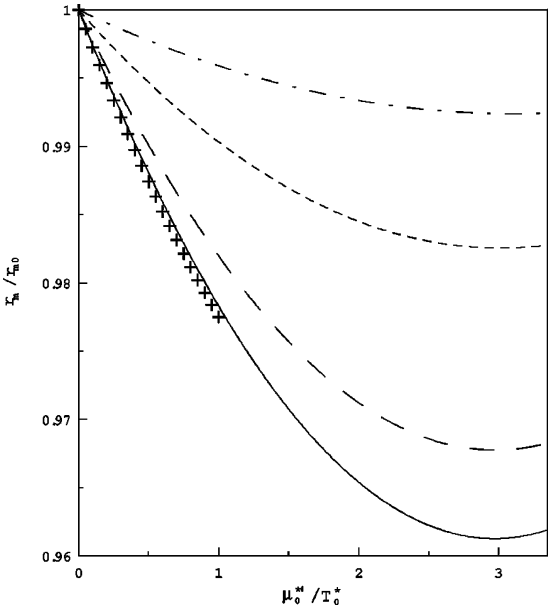

Figure 5. Relative effective diameter, $r_m/r_{m0} = f_r$, for the generalized SM interaction as a function of μ_0^{*4}/T_0^*. The lines have the same meaning as in Figure 4.

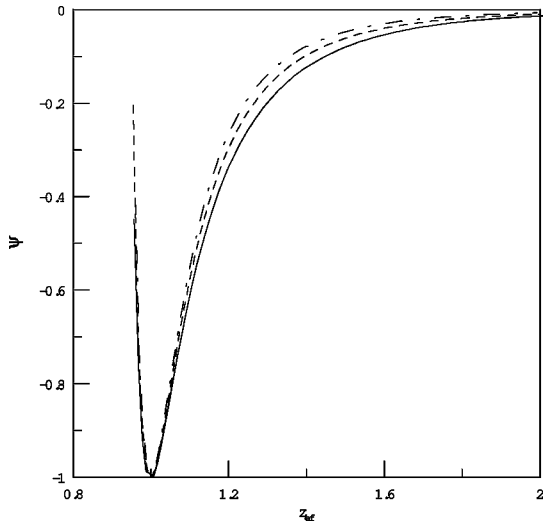

Figure 6. Form (softness) of the sphericalized potential $\psi(z_{ef})$ for the GSM interaction for $\mu_0^* = 1.0$ with $s_0 = 0.5$ at $T_0^* = 10.0$ (dashes and dots), $T_0^* = 0.8$ (short dashes) and $T_0^* = 0.3$ (continuous line). The potential $\psi(z)$ is scaled to have its minimum at $\psi(z_{ef} = 1) = -1.0$.

where $z_{ef} = r/r_m$. This potential has minimum $\psi(z_{ef} = 1) = -1$. At constant μ_0^* and s_0, the form of $\psi(z_{ef})$ against z_{ef} depends on T_0^*. This is illustrated in Figure 6: For μ_0^* and s_0 fixed, the profile of ψ against z_{ef} changes for different values of T_0^* -they only coincide at their minimum. This shows clearly that $\psi(z_{ef}; T_{01}^*)$ is nonconformal to $\psi(z_{ef}; T_{02}^* \neq T_{01}^*)$.

3.1.4. One-*s* Model. In view of previous work with real substances the one-*s* approximation should be enough to account for the interactions. To calculate s_{ef} we resort to the fact that the Boyle temperature $T_B^* = kT_B/\epsilon_0$ of an ANC system is a known function of s; i.e., $T_B^* = T_B^*(s_{ef})$.[29] Hence, knowledge of T_B^* for a given GSM system—available from the 2-*s* model or the numerical calculations—is equivalent to knowledge of its softness s_{ef} at $T_0^* = T_B^*$. Once this procedure was applied to a wide set of GSM systems with different values s_0 and μ_0^*,

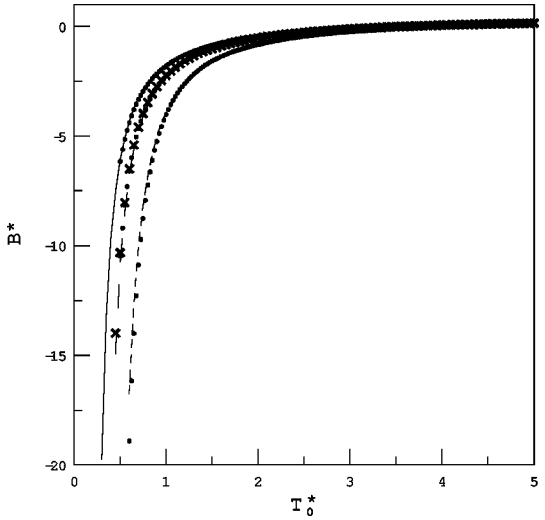

Figure 7. Test of the prediction of the second virial coefficient $B^*(T_0^*)$ of the standard SM interaction ($s_0 = s_{LJ}$, $\tilde{L} = 0$) for various dipole moments using the one-*s* approximation. The dots correspond to the numerical values of C. Vega et al.[1] The cases shown are for $\mu_0^* = 0.0$ (top), $\mu_0^* = 0.841$ (middle), and $\mu_0^* = 1.189$ (bottom). The results of the two-*s* approximation are indistinguishable from the one-*s* results at the scale of the graph.

the resulting f_s in (19) was found to follow the simple behavior

$$f_s = 1 + v(s_0)\,\mu_0^{*4}/T_0^* \tag{24}$$

where $v(s_0) = 0.44784 - 0.88078\ s_0 + 0.44504\ s_0^2 \simeq 0.44(1 - s_0)^2$. Equations 20, 21, and 24 complement eqs 17−19 in determining the effective ANC interaction. The second virial coefficient of the GSM fluid is obtained from (4) as

$$B_{GSM}^*(T_{ef}^*) = f_r^3[1 - s_{ef} + s_{ef}B_1^*(T_{ef}^*)] \tag{25}$$

with $T_{ef}^* = kT/\epsilon_{ef}$.

As an illustration, Figure 7 compares the plot of B_{GSM}^* against T_0^* for $s_0 = s_{LJ} = 1.1315$ with the numerical results of C. Vega and co-workers for three dipole strengths.[1] There is very good agreement between the ANC one-*s* model (25) and the numerical results. From the figure we can see that the model can be used to obtain $B(T)$ at lower temperatures and to interpolate for other values of μ_0^*.

The same model works for GSM molecules with $s_0 \neq s_{LJ}$. Figure 8 illustrates the behavior of $B_{GSM}^*(T_0^*)$ for $\mu_0^* = 0.8$ and various values of s_0 where it is compared with results of numerical integration of (9). Again, the model is seen to agree well with results from numerical integration. It is clear that the one-*s* model gives a very good prediction of $B(T)$ for the GSM interaction with $0.5 \leq s_0 \leq 1.13$.

4. Polar Diatomic Molecules

In this section we study the effective potentials and virial coefficients of polar diatomic molecules. A basic assumption is that a model for a polar diatomic can be built from separate contributions of polarity and elongation. The effect of polarity is accounted for by the f functions in (17), (18) and (19). The effect of the elongation of a diatomic on the effective ANC potentials has been obtained for a two-center Lennard-Jones (2-CLJ) by inversion of the second virial coefficient.[29] This

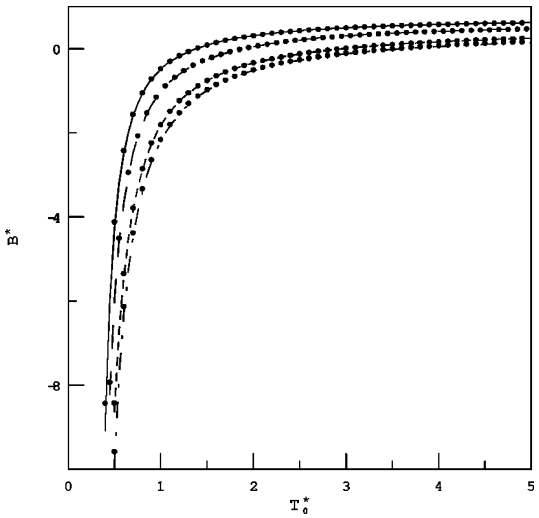

Figure 8. Effect of a variable kernel's softness, s_0, on the second virial coefficient B^* (T_0^*) of a GSM interaction ($\tilde{L} = 0$) for $\mu_0^* = 0.8$. The lines correspond to $s_0 = 0.5$ (top, continuous line), $s_0 = 0.7$ (long dashes), $s_0 = 1.0$ (short dashes), and $s_0 = 1.1315$ (bottom, dashes and dots). The lines correspond to the one-*s* approximation; the two-*s* approximation is indistinguishable from that of the one-*s* on the scale of the plot.

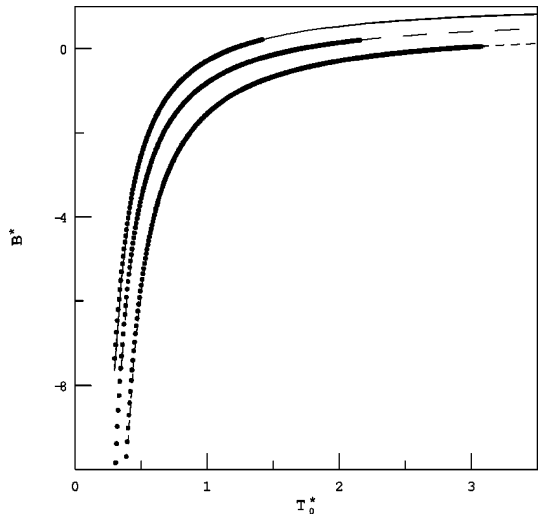

Figure 9. Predicted second virial coefficient B^* (T_0^*) of the polar LJ diatomic with $\mu_{at}^* = 0.595$ and aligned with the molecular axis, for various elongations $\tilde{L}$. The dots correspond to the numerical values of C. Vega et al.[1] The cases shown are for $\tilde{L} = 0.2$ (bottom), $\tilde{L} = 0.5$ (middle), and $\tilde{L} = 0.8$ (top). The lines correspond to the one-*s* approximation; the two-*s* approximation is indistinguishable from that of the one-*s* on the scale of the plot.

nonpolar diatomic model is further developed here due to the recent availability of very precise numerical calculations of $B(T)$.[1]

4.1. Effect of Elongation. Consider a site−site model for the interaction between two homodiatomic molecules. Let the atom−atom potential be $\varphi_{at}(r)$ where r is the distance between atoms in different molecules; $\varphi_{at}(r)$ is spherical and characterized by an energy ϵ_{at}, diameter r_{at} (at the minimum) and softness s_{at}. The elongation of a diatomic with internuclear distance l is $L^* = l/r_{at}$ or $\tilde{L} = 2^{1/6}L^*$ in terms of the van der Waals diameter used in the literature. For this diatomic $B_{dia}^* = B_{dia}/r_{at}^3 = B_{dia}^*$ (T_{at}^*; s_{at}, $\tilde{L}$) with $T_{at}^* = kT/\epsilon_{at}$. The effective *intermolecular* potential is obtained by assuming (2) to invert the $B_{dia}(T)$ data reported by C. Vega and co-workers for the 2-CLJ model with $0 \le \tilde{L} \le 10.0$.[1] The molecular parameters ϵ_{mol}, r_{mol} and s_{mol} depend on s_{at} and $\tilde{L}$ but the s_{at} dependence is very weak, so that we can safely assume that[31]

$$\epsilon_{mol} = \epsilon_{at}\, g_\epsilon(\tilde{L}) \tag{26}$$

$$r_{mol} = r_{at}\, g_r(\tilde{L}) \tag{27}$$

and

$$s_{mol} = s_{at}\, g_s(\tilde{L}) \tag{28}$$

Here $g_\epsilon(\tilde{L})$, $g_r(\tilde{L})$, and $g_s(\tilde{L})$ incorporate the effects of elongation and satisfy $\lim g_x(\tilde{L}) = 1$ when $\tilde{L} \to 0$. The $\tilde{L}$ dependence in $g_x(\tilde{L})$ is well represented by the following polynomials in $\tilde{L}$:

$$g_\epsilon = 1 - 0.363708\,\tilde{L} - 2.880128\,\tilde{L}^2 + 7.444486\,\tilde{L}^3 - 7.206996\,\tilde{L}^4 + 2.506727\,\tilde{L}^5$$

$$g_r = 1 + 0.213242\,\tilde{L} + 0205587\,\tilde{L}^2 - 0.129050\,\tilde{L}^3$$

$$g_s = (1.1315 + 0.159028\,\tilde{L} - 2.628141\,\tilde{L}^2 + 4.525942\,\tilde{L}^3 - 3.351117\,\tilde{L}^4 + 0.947182\,\tilde{L}^5)/1.1315.$$

These results improve the previous calculation of Ramos et al.[29] The resulting ϵ_{mol}, r_{mol} and s_{mol} used with (4) reproduce B_{2CLJ}^* (T^*) of Vega et al.[1] quite accurately.

4.2. Effect of the Dipoles. We consider dipoles located at the molecular centers, that is, at the midpoint of the bond between the atoms. The simplest case is when the dipole is parallel to the molecular axis; dipoles nonparallel to the axis are considered below. In a dipolar diatomic molecule the effective potential will be affected by both the dipole and the elongation of the molecular kernel. The simplest assumption is that these two factors are not correlated and can be treated separately. With this assumption, the effective potential of the dipolar diatomic is

$$u_{ef}(z_{ef}) = \varphi_{ANC}(z_{ef};\, \epsilon_{ef},\, s_{ef}) \tag{29}$$

where $z_{ef} = r/r_{ef}$ and all the necessary information has been obtained in the preceding sections. The parameters in (29) are obtained in two stages: In the first stage, (26), (28), and (27) are used to obtain s_{mol}, r_{mol}, $T_{mol}^* = T_{at}^*/g_\epsilon(\tilde{L})$, and $\mu_{mol}^{*2} = \mu_{at}^{*2}/[g_\epsilon(\tilde{L})g_r^3(\tilde{L})]$ with $\mu_{at}^{*2} = \mu^2/(\epsilon_{at}r_{at}^3)$, in terms of ϵ_{at}, s_{at}, r_{at}, and L; μ_{at}^* is a reduced "atomic" dipole moment, i.e., the dipole moment of the molecule reduced with the *atomic* parameters ϵ_{at} and r_{at}. In the second stage, equations similar to (17), (18) and (19) are used, but with T_{mol}^*, μ_{mol}^*, s_{mol}, and r_{mol} replacing T_0^*, μ_0^*, s_0 and r_{m0} respectively.

The parameters in (29) used with (25) give the virial coefficient of the polar diatomics in a explicit and closed form. Here we show predictions of $B^*(T)$ for a dipolar 2-CLJ molecule (D2CLJ) whose accuracy will be an indication of the reliability of the corresponding effective potential.

As illustration, the predicted values of B_{D2CLJ}^* against T_{at}^* for $\mu_{at}^* = 0.595$ as defined above with $\tilde{L} = 0.2$ and 0.8 are shown in Figure 9 and compared with the numerical results of Vega et al.[1] The same figure shows results of the two-*s* model; in both cases agreement is seen to be excellent. A very good agreement is maintained for $\mu_{at}^* \lesssim 0.841$ and $\tilde{L} \simeq 1.0$. We

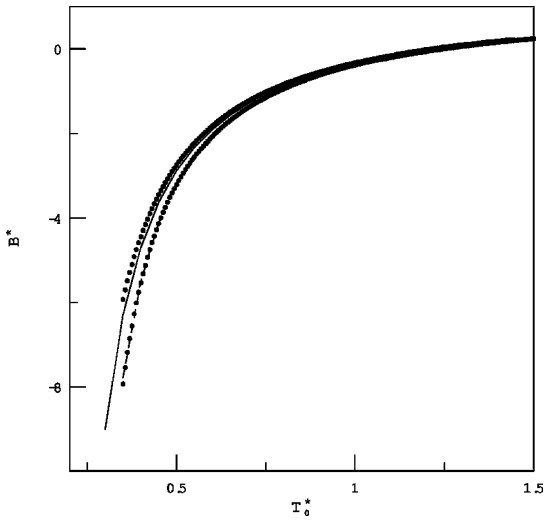

Figure 10. Test of the effective potential model for the second virial coefficient B^* (T_0^*) of the polar LJ diatomic with $\mu_{at}^* = 0.728$ and $\tilde{L} = 0.8$ at an angle α with the molecular axis. The dots correspond to the numerical values of C. Vega et al.[1] The cases shown are for $\alpha = 0.0$ (top, solid line) and $\alpha = \pi/2$ (bottom, dashed line). The lines correspond to the predictions of the one-*s* approximation; the two-*s* approximation is indistinguishable from that of the one-*s* on the scale of the plot.

expect the ANC prediction to be as accurate for $0.5 \leq s_{at} \leq 1.1$. It is then clear that the ANC model summarizes in a few expressions a very large quantity of numerical data.

4.3. Diatomics with a Nonaligned Dipole. We now consider a dipole whose axis makes an angle $\alpha \neq 0$ with the molecular axis. Figure 10 shows $B(T)$ for two D2CLJ with $\mu_{at}^* = 0.728$ and $\tilde{L} = 0.8$, the first with $\alpha = 0$ and the second with $\alpha = \pi/2$. There is a small but noticeable difference between $B(T)$ in the two cases, which means that for $\alpha \neq 0$ the effects of polarity and elongation are correlated. Unfortunately, at this moment there is no theoretical model available to calculate this correlation. So, we assumed that the effect of making $\alpha \neq 0$ on each effective parameter can be included by means of a correlation factor h_ϵ, h_r and h_s. Thus, simplified, the correlation factors depend only on μ_{at}^*, $\tilde{L}$ and α and can be evaluated by inverting the known numerical data for B_{D2CLJ}^* (T; μ_{at}^*, $\tilde{L}$,α). Explicitly, it was found that

$$\epsilon_{ef} = \epsilon_{mol} f_\epsilon(T_{mol}^*, \mu_{mol}^*, s_{mol}) h_\epsilon(\mu_{at}^*, \tilde{L}, \alpha) \quad (30)$$

$$r_{ef} = r_{mol} f_r(T_{mol}^*, \mu_{mol}^*, s_{mol}) h_r(\mu_{at}^*, \tilde{L}, \alpha) \text{ and} \quad (31)$$

$$s_{ef} = s_{mol} f_s(T_{mol}^*, \mu_{mol}^*, s_{mol}) h_s(\mu_{at}^*, \tilde{L}, \alpha) \quad (32)$$

Here ϵ_{mol}, r_{mol} and s_{mol} are again given by (26), (28), and (27) and still $L^* = l/r_{at}$. In this way we evaluated the factors h_x for $\mu_{at}^* = 0.0$, 0.420, 0.595, 0.728 and 0.841, $\tilde{L} = 0.2$, 0.4, ..., 1.0 and $\alpha = 0$, $\pi/6$, $\pi/3$, and $\pi/2$. The resulting values are smooth and well expressed by

$$h_\epsilon = 1 + d_{11}(\mu_0^*, \alpha)\tilde{L} + d_{12}(\mu_0^*, \alpha)\tilde{L}^2 \quad (33)$$

$$h_r = 1 + d_{21}(\mu_0^*, \alpha)\tilde{L} + d_{22}(\mu_0^*, \alpha)\tilde{L}^2 + d_{23}(\mu_0^*, \alpha)\tilde{L}^3 \text{ and} \quad (34)$$

$$h_s = 1 + d_{31}(\mu_0^*, \alpha)\tilde{L}^2 + d_{32}(\mu_0^*, \alpha)\tilde{L}^3 \quad (35)$$

which satisfy that $\lim h_x = 1$ when either $\tilde{L} \to 0$ or $\mu_0^* \to 0$ or $\alpha \to 0$. The coefficients $d_{ij}(\mu_0^*, \alpha)$ are, with α in radians, as follows:

$$d_{11} = -0.54889\, \mu_0^{*4} \sin(3\alpha)$$

$$d_{12} = 1.58245 \mu_0^{*4} \sin(\alpha)$$

$$d_{21} = 0.42369\, \mu_0^{*4}[\cos(\alpha) - 1]$$

$$d_{22} = -0.58675 \mu_0^{*4}[\cos(\alpha) - 1]$$

$$d_{23} = 0.51064 \mu_0^{*4}[\cos(\alpha) - 1]$$

$$d_{31} = 0.31578\, \mu_0^{*4} \sin(3\alpha)$$

$$d_{32} = 0.94301\, \mu_0^{*4} \sin(\alpha).$$

The theoretical model for $u_{ef}(z_{ef})$ and $B(T)$ for the polar diatomic is given, as before, by (29) and (25) but now the parameters are given by (30), (31), and (32). As a last check on the functions h_x, the virial coefficient B_{D2CLJ}^* (T; μ_{at}^*, $\tilde{L}$, $\alpha = \pi/2$) is compared in Figure 10 with the original numerical results[1] for $\mu_{at}^* = 0.728$ and $\tilde{L} = 0.8$; the case $\alpha = 0$ is also shown as reference.

5. Applications at Finite Density

The main assumption is that at finite densities the effective potential of the polar fluid is still given by an ANC function. In a first approximation, φ_{ANC} is taken to be independent of density. The equation of state and critical properties of ANC fluids have been studied by *NVT* and Gibbs ensemble Monte Carlo simulations[33,46] Here we quote only the relevant results. The reduced critical temperature $T_c^* = kT_c/\epsilon_c$, pressure $P_c^* = P_c r_c^3/\epsilon_c$ and density $\rho_c^* = \rho_c r_c^3$ of the ANC fluid are solely a function of s_c. We have written ϵ_c, r_c, and s_c to stress that they are evaluated at the critical point. For $0.5 \leq s \leq 1.2$ they have been found to be given by

$$kT_c/\epsilon_c = 0.348915 + 0.326038 s_c + 0.443771 s_c^2 \quad (36)$$

$$\rho_c r_c^3 = 0.74226 \quad (37)$$

$$P_c r_c^3/\epsilon_c = -4.2179 + 25.1353\, s_c \quad (38)$$

where ϵ_c/k and r_c are given in K and Å, respectively, whereas T_c, ρ_c and P_c are given in K, mol/cm^3, and atm, respectively. It must be pointed out that ρ_c^* is independent of s_c.

5.1. Critical Temperature of Stockmayer Fluids. A thorough investigation of the applicability of this model potential to the equation of state of a Stockmayer fluid, including a critical comparison with the equation of state proposed by Szalai and co-workers,[16] is currently under way. As a first application we calculate the effect of the dipolar interaction on the critical temperature of a dipolar GSM fluid. The critical temperature, reduced with the kernel parameters, is $T_{0c}^* = kT_c/\epsilon_0 = T_c^* \times (\epsilon_c/\epsilon_0)$ and for the GSM model is obtained from (36) by substituting $\epsilon_c = \epsilon$ from (17) and s_c from (24). Therefore, with fixed μ_0^* and s_0, T_{0c}^* is obtained by solving the simultaneous equations

$$T_{0c}^* = T_c^*(s) f_\epsilon(T_{0c}^*, \mu_0^*, s_0)$$

$$s = s_0 f_s(T_{0c}^*, \mu_0^*, s_0)$$

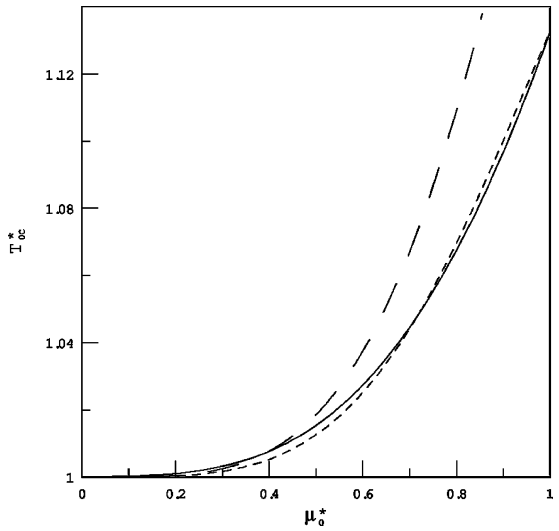

Figure 11. Critical temperature of the standard Stockmayer fluid, $s_0 = s_{LJ}$, as a function of dipolar strength μ_0^*. The prediction with the effective potential of this work (long-dashed line) is compared with the fit of the simulation results of van Leeuwen (short-dashed line).[38] The continuous line gives the ANC result including the empirical correction on ϵ_c by the factor j_ϵ as discussed in the text.

leading to a third-order equation in T_{0c}^*. Its real solution leads to the desired relation

$$T_{0c}^* = T_{0c}^*(\mu_0^*, s_0) \tag{39}$$

where $T_{0c}^*(\mu_0^*, s_0)$ is an explicit but complicated function of μ_0^{*2} with coefficients dependent on s_0.

Equation 39 predicts that, at constant s_0, T_{0c}^* increases with μ_0^*. This is illustrated in Figure 11 for the standard SM case $s_0 = s_{LJ}$ where this model is compared with the results of Gibbs ensemble simulations (GEMC) for a SM fluid with $0 \le \mu_0^* \le 1.0$.[36−38] As seen in this figure, the effective potential model predicts correctly the trend of the simulation results although overestimating the effect of the dipoles. This is a limitation of having assumed ϵ to be density independent and thus using for ϵ_c the zero density limit (17). At small densities the most probable orientation between two dipoles is the antiparallel orientation but at finite densities there is an effect caused by correlations with other particles; it is perhaps this the mechanism which makes $\epsilon_c < \epsilon_0$. To estimate this effect on ϵ_c, we use the fact that $s =$ constant is a good approximation for the LJ kernel at all densities[33] and thus keep $s_0 = s_{LJ}$. This allows us to use the LJ equation of state to calculate the value of ϵ_c that leads to the observed T_{0c}^*. By applying this procedure to a few values of μ_0^* it is found that ϵ in eq 17 should be corrected by a factor $j_\epsilon = 1 + c_\epsilon \rho_0^* \mu_0^{*4}$ where $c_\epsilon \simeq -0.20$ is constant and $\rho_0^* = \rho r_{m0}{}^3$. This semiempirical correction reduces the value of ϵ_c and thus that of T_{0c}^* in agreement with the GEMC results for the SM fluid for $\mu_0^* \le 1.2$.

5.2. HCl: Example of a Real Polar Molecule. Here we consider a typical real polar substance, HCl, and show that the ANC theory gives a coherent picture of fluid HCl at low and finite densities. In this application we follow a route inverse to that of the previous application. Assuming again an ANC potential to be valid, we will first determine ϵ_c, r_c, and s_c from the critical properties of HCl and from them obtain the kernel's parameters in the dilute gas, ϵ_0, r_{m0}, and s_0. Then we show that these parameters lead to a second virial coefficient that agrees very well with experiment.

For HCl, the values $T_c = 324.7$ K, $V_c = 81$ cm^3/mol $= 1/\rho_c$, and $P_c = 82$ atm were taken from the compilation of Ambrose.[47] Solving eqs 36−38 for the effective parameters at the critical point, we found $\epsilon_c/k = 468.9$ K, $r_c = 3.918$ Å, and $s_c = 0.5861$. This value of ϵ_c includes the effect of the dipolar interaction.

Nevertheless, in real fluids such as HCl there appear additional effects of which two are perhaps the most relevant. The first is the effect of correlations on the statistical averaging which introduces a density dependence as discussed in the previous subsection. The second is the presence, at finite densities, of many-body forces that do not act in the dilute gas state. Since the above procedure is based on experimentally determined T_c, V_c, and P_c the parameters ϵ_K, r_K, and s_K contain all these effects. Of the many-body forces, the most important is the three-body force of the Axilrod−Teller (AT) type.[33] The net effect of the AT force is to add a repulsion between the molecules, thereby producing a shallower well. This means that the value of ϵ_0/k foe HCl at low densities, where it is not affected by multiple-body effects, should be larger than $\epsilon_K/k = 468.9$ K just calculated. The effect of the AT forces has been exhibited, among others, by Anta and co-workers for the case of argon.[48] Inclusion of the AT term, additional to an accurate two-body term, is necessary to make a quantitatively good prediction of the orthobaric curve of argon. From the results of Anta et al.'s work one finds that $\epsilon_0/\epsilon_c \cong 1.07$ although other terms would have a smaller additional effect. Besides, this same effect appears when T_c and ρ_c of real substances are reduced with the low-density ANC parameters ϵ_0, r_{m0}, and s_0. Indeed, it has been shown that they satisfy to a good approximation the following correlations[32]

$$kT_c/\epsilon_0 = 0.1206337 + 0.759946 s_0 + 0.151390 s_0{}^2 \tag{40}$$

$$\rho_c r_{m0}{}^3 = 0.426 \tag{41}$$

where ρ_c is given in particles/Å^3. As for the shape factor s, it has been found that it is little affceted by either the presence of correlations (as in the GSM model) or of AT forces. The difference between eqs 36 and 37 and eqs 40 and 41 is a measure of the many-body and correlation effects on the effective potentials. For instance, calculating ϵ_0/ϵ_c from (36) and (40) and taking $s_0 = 1.0$, one finds $\epsilon_0/\epsilon_c = 1.08$ for argon, very close to Anta et al.'s value.

Using eqs 40 and 41 and assuming that $s_c = s_0$, we found that the values of the HCl effective parameters at low density are $\epsilon_0/k = 525.4$ K, $r_{m0} = 3.855$ Å, and $s_0 = 0.5861$. This gives $\epsilon_0/\epsilon_c = 1.12$ for HCl being bigger than for argon but of the same order of magnitude.

The next step is to obtain the kernel parameters at zero density that will be denoted by ϵ_K, r_K, and s_K. Since HCl is not an elongated molecule, we assume its kernel to be spherical and hence use the ANC model for the GSM fluid. Hence eqs 17, 18, and 24 are rewritten as $\epsilon_0 = \epsilon_K f_\epsilon$, $r_{m0} = r_K f_r$, and $s_0 = s_K f_s$, and taking $\mu = 1.08$ D,[49] we obtain finally the kernel parameters $\epsilon_K/k = 501.9$, $r_K = 3.859$ Å, and $s_K = 0.579$.

These values have been used with the GSM model to predict the second virial coefficient of HCl. The result is shown in Figure 12 where it is compared with experimental data with excellent agreement over the whole range for which experimental data are available.[50] This range is 190 K $\le T \le$ 480 K to be compared with the normal melting point of HCl at 114.8 K and critical temperature at 324.7 K. For comparison, the same figure includes the empirical correlation due to Tsonopoulos as reported by Weber.[51]

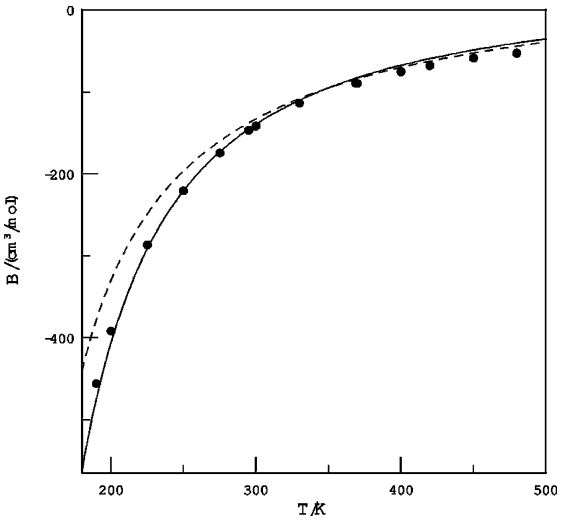

Figure 12. Test of the effective potential model to predict the second virial coefficient $B(T)$ of HCl. The dots correspond to experimental data, the solid line is the ANC prediction and the dashed line is Tsonopoulos' correlation.

5.3. Conclusions. We have built a model for an effective spherical potential of polar molecules. The resulting interaction has the form of an ANC potential whose parameters—energy ϵ_{ef}, diameter r_{mef} and softness s_{ef}—depend on the dipole moment of the molecules, on the diameter and softness of its kernel—i.e. its nonpolar part—and, for diatomic kernels, on its elongation.

The potential model developed in this work is able to predict the second virial coefficients $B(T)$ of dipolar molecules, both with spherical and nonspherical kernels. These predictions agree very well, for $\mu_0^* \lesssim 1.0$, with the numerical calculations of C. Vega et al. in the cases of Stockmayer molecules and of polar 2-CLJ diatomics. Thus, this model synthesizes accurately and in closed form a great part of the extensive numerical data of $B(T)$ for dipolar 2-CLJ molecules already available.

The model can be used also for dipolar molecules whose kernels are nonconformal to a LJ-12/6 function. Since many real nonpolar molecules has been shown to be notably nonconformal to LJ, the model presented here should effectively represent dipolar interactions more flexibly, accurately, and simply. These model potentials, developed in the dilute gaseous phase, are being used to predict thermodynamic properties of polar fluids at liquidlike densities. Here we present as illustrations the prediction of the critical temperature of Stockmayer molecules and, for the HCl molecule, a prediction of its virial coefficient based on knowledge of its critical properties.

Acknowledgment. The authors are grateful to Dr. Carlos Vega, Universidad Complutense, Madrid, for providing useful details about the second virial calculations of dipolar 2-CLJ molecules. E.Á. thanks Conacyt (México) for the scholarship granted for his Ph.D. studies and to the Universidad Pablo de Olavide for support during a stay.

Appendix

A.1. ANC Two-*s* Approximation. A second-order ANC approximation considers that $s = \langle S(\varphi, \Omega)\rangle$ differs in the attractive $z < 1$ and repulsive $z > 1$ parts of $\varphi(z, \Omega)$; the ANC potential is still defined by eq 2 but with $s = s_A$ for $z < 1$ and $s = s_R$ for $z > 1$. The virial coefficient $B(T)$ written in terms of s_A and s_R, and properties of the reference is given in the original papers.[29] Adding a dipolar interaction to the spherical kernel alters its softness s_0 by factors f_{s_A} for $z > 1$ and f_{s_R} for $z < 1$, so that $s_A = s_0\, f_{s_A}(T_0^*, \mu_0^*, s_0)$ and $s_R = s_0\, f_{s_R}(T_0^*, \mu_0^*, s_0)$.

Calculation of f_{s_A}. Let $s_{A0} = s_A(T_0^*)$ be the softness of $\psi(z; T_0^*)$ at a fixed T_0^*; s_{A0} is given by[29]

$$\Lambda_0^*(T^*) = 1 - s_{A0} + s_{A0}\Lambda_1^*(T^*) \tag{A.1}$$

where Λ_1^* is the (known) reference volume and

$$\Lambda_0^*(T^*) = 1 + \frac{3}{\exp(1/T^*) - 1}\int_1^\infty dz\, z^2\{\exp[-\psi(z; T_0^*)/T^*] - 1\} \tag{A.2}$$

Use of (A.2) for T_0^* fixed and a chosen value of T^* gives $\Lambda_0^*(T^*)$, which substituted in (A.1) gives one value of s_{A0}. Since s_{A0} is slightly dependent on the T^* chosen, its final value was taken as the average of its values at $T^* = 0.5$ and $T^* = 5.0$. This procedure was applied for $0.3 \le T_0^* < 10.0$ and $s_A(T_0^*)$ was obtained for $\mu_0^* = 0.25$, 0.5, 0.75, 0.9, and 1.0 and $s_0 =$ 0.5, 0.7, 0.8, 0.9, and 1.0. The data of s_A was used to fit the expression

$$f_{s_A} = 1 + p_1(s_0)\mu_0^{*4}/T_0^* + p_2(s_0)\mu_0^{*6}/T_0^{*2} \tag{A.3}$$

where the polynomials $p_i(s_0)$ are given below. Equation A.3 reproduces adequately the dependence of s_A on T_0^* and μ_0^*.

Calculation of f_{s_R}. The factor f_{s_R} is treated in a way similar to f_{s_A}. The relationship analogous to (A.1) involves now $s_{R0} = s_R(T_0^*)$ and $b_0^*(T^*)$ given by

$$b_0^*(T^*) = 1 - 3\exp(-1/T^*)\int_0^1 dz\, z^2\exp[-\psi(z; T_0^*)/T^*].$$

The expression found finally for f_{s_R} is

$$f_{s_R} = 1 + q_1(s_0)\mu_0^{*4}/T_0^* + q_2(s_0)\mu_0^{*6}/T_0^{*2} + q_3(s_0)\mu_0^{*8}/T_0^{*3} + q_4(s_0)\mu_0^{*10}/T_0^{*4} \tag{A.4}$$

the cubic polynomials $q_1(s_0)$ are given next.

The polynomials determining the factors f_s^A and f_s^R in (A.3) and (A.4) are

$$p_1 = (0.2734 - 0.4677s_0 + 0.2087s_0^2)/s_0$$

$$p_2 = -(0.06087 - 0.1582s_0 + 0.1042s_0^2)/s_0$$

and

$$q_1 = (0.05736 - 0.14846s_0 + 0.13886s_0^2)/s_0$$

$$q_2 = -(0.08549 - 0.2253s_0 + 0.2198s_0^2)/s_0$$

$$q_3 = (0.05724 - 0.1546s_0 + 0.1407s_0^2)/s_0$$

$$q_4 = -(0.01218 - 0.03365s_0 + 0.02856s_0^2)/s_0.$$

The effective potential of the generalized Stockmayer potential is now $u_{ef}(z_{ef}) = \varphi_{ANC}(z_{ef}; \epsilon_{ef}, s_{ef}^R, s_{ef}^A)$ where $s_{ef}^R = s_0 f_{s_R}$ and $s_{ef}^A = s_0 f_{s_A}$. This potential gives the second virial coefficient of the GSM gas

$$B_{GSM}^*(T_0^*; s_0, \mu_0^*) = B_{ANC}^*(T_{ef}^*; f_r, s_{ef}^R, s_{ef}^A)$$

This more precise approximation was used in inverting the $B_{D2CLJ}^*(T)$ data[1] at fixed μ_{at}^*, $\tilde{L}$, and α.

A.2. Sphericalization of $\varphi_{DD}(\Omega)$ and Analytic Form of $B(T)$ for GSM. The dipole−dipole interaction is written as

$$\varphi_{DD}(z, \Omega)/\epsilon_0 = -\mu_0^{*2} g(\Omega)/z^3$$

where $\mu_0^{*2} = \mu^2/\epsilon_0 r_{m0}^3$ and

$$g(\Omega) = 2\cos\theta_1\cos\theta_2 - \sin\theta_1\sin\theta_2\cos(\phi_2 - \phi_1) \quad (A.5)$$

Here θ_i and ϕ_i are the zenithal and azimuthal angles of the dipole on molecule i. We follow Hirschfelder et al.[41] and factorize $\exp(-\varphi_{GSM}/\epsilon_0 T_0^*)$, expand $\exp(\varphi_{DD}/\epsilon_0 T_0^*)$, and integrate over Ω, and we find

$$\frac{1}{8\pi}\int d\Omega \exp(-\varphi_{DD}(z, \Omega)/\epsilon_0 T_0^*) = \sum_{m=0}^{\infty}\left\{\frac{1}{(2m)!}[\mu_0^{*2}/T_0^* z^3]^{2m} G_m\right\}$$

where the constant coefficients

$$G_m = (1/8\pi)\int d\Omega\, [g(\Omega)]^{2m} \quad (A.6)$$

may be calculated analytically for m finite using $g(\Omega)$ from (A.5).

We now give the analytic result for $B(T)$ of the GSM potential with $s_0 = 1$, identical to a SM function with a spherical Kihara as kernel, i.e.

$$\varphi_K(z) = \epsilon\left[\left(\frac{1-a}{z-a}\right)^{12} - 2\left(\frac{1-a}{z-a}\right)^{6}\right] \quad (A.7)$$

To obtain $B(T)$ of $\varphi_{GSM}^{sphe}(z; s_0 = 1)$ we perform the integral over z in (9) in a way similar to that used by Hirshfelder et al.[41] and get

$$B^*(T^*, \mu_0^*) = -\sum_{n=0}^{\infty}\sum_{k=0}^{k\le n/2}\sum_{l=0}^{\infty}\frac{2^n - 2k}{n!}\frac{a^l}{(1-a)^{6k+1}}\left(\frac{1}{T^*}\right)^{6n+6k-l/12}\times\begin{bmatrix} n \\ 2k\end{bmatrix}\begin{bmatrix} 6k \\ l\end{bmatrix}\mu_0^* G_k\left\{(1-a)^3\frac{1}{4}\left(\frac{1}{T^*}\right)^{1/4}\times\Gamma\left(\frac{6n-6k+l-3}{12}\right) + (1-a)^2 a\frac{1}{2}\left(\frac{1}{T^*}\right)^{1/6}\times\Gamma\left(\frac{6n-6k+l-2}{12}\right) + (1-a)a^2\frac{1}{4}\left(\frac{1}{T^*}\right)^{1/12}\times\Gamma\left(\frac{6n-6k+l-1}{12}\right)\right\} \quad (A.8)$$

where $\binom{2k}{n}$ is the coefficient of the binomial Newton expansion, $\Gamma(\cdot)$ is the gamma function, G_k is the same as in (A.6) and

$$\begin{bmatrix} 6k \\ l\end{bmatrix} = (-1)^l\frac{(6k+l-1)!}{l!(6k-1)!}$$

Truncation of the series on the right-hand side of eq A.8 allows one to calculate $B(T)$ to any desired accuracy. Moreover, taking $a = 0$ in (A.7) makes $\varphi_K(z) = \varphi_{LJ}(z)$ so that we recover the well-known standard SM result.[41]

References and Notes

(1) Vega, C.; McBride, C.; Menduiña, C. *Phys. Chem. Chem. Phys.* **2002**, *4*, 3000.
(2) Wertheim, M. S. *Annu. Rev. Phys. Chem.* **1979**, *30*, 471.
(3) Rossky, P. J. *Annu. Rev. Phys. Chem.* **1985**, *36*, 321.
(4) Teixeira, P. I. C.; Tavares, J. M.; Telo da Gama, M. M. *J. Phys.: Condens. Matter*. **2000**, *12*, R411.
(5) van Leeuwen, M. E.; Smit, B. *Phys. Rev. Lett.* **1993**, *71*, 3991.
(6) Levesque, D.; Weis, J. J. *Phys. Rev. E* **1994**, *49*, 5131.
(7) Tavares, J. M.; Weis, J. J.; Telo da Gama, M. M. *Phys. Rev. E* **1999**, *59*, 4388.
(8) Spöler, C.; Klapp, S. H. L. *J. Chem. Phys.* **2003**, *118*, 3628.
(9) Allen, P. B. *J. Chem. Phys.* **2004**, *120*, 2951.
(10) Vega, C.; Lago, S. *J. Chem. Phys.* **1994**, *100*, 6727.
(11) McGrother, S. C.; Gil-Villegas, A.; Jackson, G. *J. Phys.: Condens. Matter* **1996**, *8*, 9649.
(12) Williamson, D. C.; del Río, F. *J. Chem. Phys.* **1997**, *107*, 21.
(13) Lago, S.; Lopez-Vidal, S.; Garzon, B.; Mejias, J. A.; Anta, J. A.; Calero, S. *Phys. Rev. E* **2003**, *68*, 021201.
(14) Chen, X. S.; Fortsmann, F.; Katsch, M. *J. Chem. Phys.* **1991**, *95*, 2832.
(15) Benavides, A. L.; Guevara, Y.; del Río, F. *Physica A* **1994**, *202*, 420.
(16) Szalai, I.; Kronome, G.; Lukács, T. *J. Chem. Soc., Faraday Trans.* **1997**, *93*, 3737.
(17) Szalai, I.; Henderson, D.; Boda, D.; Chan, K. Y. *J. Chem. Phys.* **1999**, *111*, 337.
(18) Gil-Villegas, A.; del Río, F.; Vega, C. *Phys. Rev. E.* **1996**, *53*, 2326.
(19) Attard, P. *Phys. Rev.* A **1992**, *45*, 3659.
(20) van der Hoef, M. A.; Madden, P. A. *J. Chem. Phys.* **1999**, *111*, 520.
(21) McMillan, W. G.; Mayer, J. E. *J. Chem. Phys.* **1945**, *13*, 276.
(22) Rowlinson, J. S. *Mol. Phys.* **1984**, *52*, 567.
(23) del Río, F. *Mol. Phys.* **1992**, *76*, 21.
(24) Louis, A. A. *J. Phys.: Condens. Matter* **2002**, *14*, 9187.
(25) Stillinger, F. H.; Sakai, H.; Torcuato, S. *J. Chem. Phys.* **2002**, *117*, 288.
(26) Anta, J. A.; Bresme, F.; Lago, S. *J. Phys.: Condens. Matter* **2003**, *15*, S3491.
(27) del Río, F. *Mol. Phys.* **1981**, *42*, 217.
(28) del Río, F.; Ramos, J. E.; McLure, I. A. *J. Phys. Chem.* B **1998**, *102*, 10568.
(29) Ramos, J. E.; del Río, F.; McLure, I. A. *J. Phys. Chem.* B **1998**, *102*, 10576.
(30) McLure, I. A.; Ramos, J. E.; del Río, F. *J. Phys. Chem. B* **1999**, *103*, 7019.
(31) del Río, F.; Ramos, J. E.; McLure, I. A. *Phys. Chem. Chem. Phys.* **1999**, *1*, 4937; **2000**, *2*, 2731.
(32) Ramos, J. E.; del Río, F.; McLure, I. A. *Phys. Chem. Chem. Phys.* **2001**, *3*, 2634.
(33) Guzmán, O.; del Río, F. *J. Phys. Chem.* B **2001**, *105*, 8220.
(34) del Río, F.; Ibarra, B. *Mol. Phys.* **2003**, *101*, 2997.
(35) Müller, E. A.; Gelb, L. D. *Ind. Eng. Chem. Res.* **2003**, *42*, 4123.
(36) Smit, B.; Williams, C. P.; Hendriks, E. M.; de Leew, S. W. *Mol. Phys.* **1989**, *68*, 765.
(37) van Leeuwen, M. E.; Smit, B.; Hendriks, E. M. *Mol. Phys.* **1993**, *78*, 271.
(38) van Leeuwen, M. E. *Mol. Phys.* **1994**, *82*, 383.
(39) Ramos, J. E.; del Río, F.; McLure, I. A. *Phys. Chem. Chem. Phys.* **2001**, *2*, 2731.
(40) del Río, F.; Ávalos, E. *Developments in Mathematical and Experimental Physics*; Kluwer Academic/Plenum Publishers: México City, 2003; Volume B: Statistical Physics and Beyond, p 253.
(41) Hirschfelder, J. O.; Curtiss, C. F.; Bird, R. B. *Molecular Theory of Gases and Liquids*, John Wiley & Sons: New York, 1954, Chapter 3.
(42) Massih, A. R.; Mansoori, G. A. *Fluid Phase Equilibr.* **1983**, *10*, 57.
(43) French, R. H. *J. Am. Ceram. Soc.* **2000**, *83*, 9.
(44) Boublık, T. *Collect. Czech. Chem. Commun.* **1994**, *59*, 756.
(45) van Leeuwen, M. E. *Fluid Phase Equilibr* **1994**, *99*, 1.
(46) Ramos, J. E. Ph.D. Thesis, University Aut. Metr., México City, 2002.
(47) Ambrose, D. *Vapour-Liquid critical Properties*; National Physical Laboratory, London, U.K., 1983.
(48) Anta, J. A.; Lomba, E.; Lombardero, M. *Phys. Rev. E* **1997**, *55*, 2707.
(49) Poling, B. R.; Prausnitz, J. M.; O'Connell, J. P. *Properties of Gases and Liquids*; McGraw-Hill: New York, 2001.
(50) Dymond, J. H.; Smith, E. B. *Virial coefficients of pure gases and mixtures*; Clarendon Press: Oxford, U.K., 1980.
(51) Weber, L. A. *Int. J. Thermophys.* **1994**, *15*, 461.